Journal of Applied Polymer Science

Improvement of the Adhesion Properties of Silicone Rubber by the Incorporation of Silane-Modified Montmorillonite

Eung Soo Kim, Eun Jeong Kim, Tae Hwa Lee, Jin San Yoon
Department of Polymer Science and Engineering, Inha University, Yonghyun-Dong, Nam-Gu, Incheon 402-751, Korea
Correspondence to: J. S. Yoon (E mail: jsyoon@inha.ac.kr)

ABSTRACT: A silicone rubber precursor was amended by the incorporation of γ-aminopropyl triethoxysilane (APS) into siloxane to prepare an elastomeric thermal insulator adhering to the isocyanate-group-containing liner sheets, which are actually used to envelop rocket propellants. This improved adhesion may protect the liners of the rocket motor cases efficiently against the hot combustion gas. Clay was modified by cationic exchange with an amine compound, and the resulting clay was further treated with APS and *N*-(2-aminoethyl)-3-aminopropyl trimethoxysilane to introduce amine groups onto the surface of the clay to further improve the adhesion of the silicone rubber to the liner. The neat and modified clays were compounded with the APS-amended silicone rubber [room-temperature vulcanizate (RTV)]. The effects of the clay modification on the adhesion properties were explored. The peel strength between the liner and the room-temperature silicone rubber (RTV) based on siloxane was 0, whereas the peel strength increased to 3.7 N/cm when the silicone rubber was amended with APS. The peel strength between APS–RTV and the liner was lower than 3.7 N/cm when clay was added, whereas the peel strength became higher than 5.7 N/cm so that APS–RTV could not withstand the peeling force and was torn off before the delamination when the amine silane modified clay was added instead of clay. © 2012 Wiley Periodicals, Inc. J. Appl. Polym. Sci. 128: 2563–2570, 2013

KEYWORDS: adhesion; clay; silicones

Received 23 January 2012; accepted 8 July 2012; published online 9 November 2012
DOI: 10.1002/app.38489

INTRODUCTION

Rocket motor cases need to be protected from the sizzling temperatures generated by propellant combustion.[1,2] Usually, a thermally stable type of rubber is sandwiched between the rocket motor case and the liner covering the rocket propellant.[3] The rubber should not only exhibit a good thermal stability but should also adhere to the liner and to the motor case closely and strongly enough so that hot combustion gas does not circulate through the interstices, if any, because this will raise the combustion temperature uncontrollably and eventually to lead to the explosion of the rocket motor.[4] The insulating rubber should also have good mechanical properties to withstand the shear caused by the high velocity (ca. Mach 0.02–10) combustion gas.[5–7] Silicone rubber possesses excellent physical and chemical properties.[8–11] It remains flexible and preserves its stress–strain properties over a broad range of temperatures for an extended period of time. However, silicone rubber has an extremely low surface tension, which can lead to poor adhesive properties.[12,13] Therefore, its adhesive properties should be greatly improved so that it can be used as a thermal insulator for rocket motors.[14,15]

Because the liner components contain dimeric diisocyanate (DDI) as a crosslinker, the introduction of amine groups, which are highly reactive toward the isocyanate group, through the copolymerization of γ-aminopropyl triethoxysilane (APS) with dimethyl siloxane may produce silicone rubbers with good adhesion properties to the liner.[16]

Clays have a high aspect ratio, and thereby, the advanced performance of polymeric materials can be achieved by the incorporation of a much smaller amount of clay compared to that of conventional micrometer-scale fillers. Because clays are hydrophilic in nature, they should be modified to raise their compatibility with hydrophobic polymer matrices.[17–20] The organomodification of clay is a crucial step in the preparation of polymer/clay composites. A good dispersion of the clay layers in the polymer matrix and strong interactions between the clay layers and the polymer matrix are needed to obtain polymer/clay composites with superior mechanical properties. Various modification techniques have been used to enhance the interactions and degree of dispersion of the clay layers.[21]

In a previous article,[16] we reported that the incorporation of APS into hydroxyl-terminated polydimethylsiloxane (PDMS)

Table I. Recipes for the Preparation of the APS–RTV Composites

	Clay (wt %)			CBM (wt %)	Silane (wt %)		Catalyst (wt %)
Composite	MMT	APC	ZC	N200 series	APS	TPOS	Tin
APS-RTV	—	—	—	2	2	10	0.1
APS-RTV/MMT	2	—	—	2	2	10	0.1
APS-RTV/DAPC	—	2	—	2	2	10	0.1
APS-RTV/DZC	—	—	2	2	2	10	0.1

silicone rubber contributed to the adhesion between the silicone rubber and the liner. This was rationalized by the enhancement of the interaction between the two sheets due to the chemical reaction between the amine group of APS and the isocyanate (-NCO) groups in the liner to yield a urethane linkage. However, a long time was needed for curing at room temperature to achieve an adhesion strength great enough for the rubber to be used safely as an insulation rubber for rocket motors.

In this study, we attempted to accelerate and further improve this adhesion by adding clays endowed with amine groups to the silicone rubber. The clays were modified not only through the cation-exchange reaction but also through the grafting of silane compounds bearing amine groups to the clays. The improvements in the adhesion properties were explored as a function of the clay modification method.

EXPERIMENTAL

Materials

PDMS that contained 12% precipitated silica was purchased from Dong-Yang Silicone (Icksan, Korea). This compound was a room-temperature, vulcanization-type silicone rubber. Tetrapropoxysilane (TPOS; Aldrich, St. Louis, MO) and APS (Aldrich) were added to the silicone rubber as a crosslinking agent and an adhesion promotion agent, respectively. Carbon black (CB; model MA100, N200 series) was also supplied by Dong Yang Silicone. The CB particles were about 10–20 nm in diameter. Because CB particles tend to be aggregated, they could not disperse in the room-temperature vulcanizate (RTV). Therefore, the CB particles were premixed into PDMS of low viscosity (200 cps) to prepare a homogeneous carbon black master batch (CBM), which was then mixed with RTV until a well-dispersed mixture with a 2 wt % CB content was obtained. The sample recipe is listed in Table I.

The liner components included hydroxyl-terminated polybutadiene (HTPB), DDI as a crosslinker, and ferric acetyl acetonate (FeAA) as a catalyst and were supplied by the Agency for Defense Development (Daejeon, Korea). Dioctyl adipate and *N*-991 CB were included in HTPB as a plasticizer and a filler, respectively. Sodium montmorillonite (MMT) was purchased from Southern Clay Products (Gonzales, TX). 1,12-Diaminododecane (12DA; Aldrich), APS (Aldrich), and *N*-(2-aminoethyl)-3-aminopropyltrimethoxysilane (Z6020, Dow Corning, Jincheon, Korea) were used for the modification of the clay.

Clay Modification

MMT (20 g) was suspended in 1 L of distilled water and was then introduced into a reactor whose temperature was raised to 65°C with stirring. Then, 9 mmol of 12DA and 18 mmol of HCl aqueous solution were added to the mixture, which was then stirred vigorously for 12 h. The precipitate was isolated by filtration after purification with hot water. The 1,12-diaminododecane-modified clay (12DAC) was dried under reduced pressure at 60°C for 48 h and then ground into 50-μm particles. 12DAC was treated with two kinds of silanes, APS and Z6020, to prepare DAPC (APS-modified 12DAC) and DZC (Z6020-modified 12DAC), respectively. After APS or Z6020 was mixed with a 13 : 7 w/w methanol/deionized water mixture at 65°C, 12DAC was added to the mixture under reflux for 12 h. The product was washed and filtered with ethanol several times at room temperature to remove the unreacted silane compound. The product was dried in a vacuum oven at 60°C for at least 48 h. The modified clays were ground into powder with particles 50 μm in size. MMT was also modified with APS and Z6020 but in the absence of 12DA to make reference clays that were named APC (APS-modified MMT) and ZC (Z6020-modified MMT), respectively.

Preparation of Silicone Rubber

An RTV silicone rubber sheet was prepared from hydroxyl-terminated PDMS and TPOS in the bulk state with dibutyl tin dilaurate (0.1 wt %, Aldrich) as a catalyst. RTV was completely dissolved in toluene (1 : 3 weight ratio) at room temperature, and the resulting mixture was then mixed with 10% crosslinker and 2.0 wt % APS. The clay or the modified clay (2 wt %) was also added to the mixture when needed. The mixture was dried at room temperature for 48 h and then cured in a convection oven at 60°C for 72 h in a suitable molder with dimensions of $10 \times 20 \times 2$ cm^3.

Preparation of the Liner and Peel Test Specimens

The liner sheet was prepared with a mixture composed of HTPB, DDI, and FeAA (at a weight ratio of 88.7 : 11.3 : 0.05). The mixture was spread to about 3 mm in thickness on the silicone rubber sheet, which was prepared as described previously. The mixture was then cured at room temperature for 24 h. After the curing of the silicone rubber sheet, the liner mixture to be cured was spread onto the silicone rubber sheet and cured at 60°C for 72 h to prepare the specimens for measurement of the adhesion properties through the peeling test. The sample preparation procedure is described in Scheme 1.

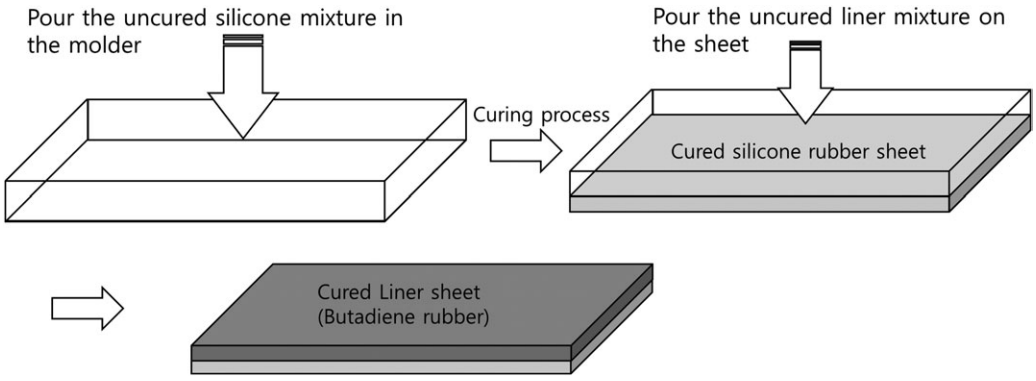

Scheme 1. Creation process of the assembled rubber sheet.

Measurements

Fourier transform infrared (FTIR) spectroscopy results were obtained with a VERTEX 80V infrared spectrometer (Bruker, Ettlingen, Germany). The FTIR spectra were recorded in a wavenumber range of 4000–400 cm^{-1} in transmission mode. These data were scanned at least 5000 times to obtain the spectra. Thermal analyses of the silicone rubber and the APS–RTV/clay composites were performed with thermogravimetric analysis (TGA; Q50, TA instruments, New Castle, DE). The sample size was about 10–20 mg. The samples were heated at 20°C/min from 25 to 800°C under a dry nitrogen flow at 90 cm^3/min. The X-ray diffraction (XRD) measurements were carried out with a Rigaku DMAX 2500 X-ray diffractometer with reflection geometry and Cu Kα radiation and operating at 40 kV and 100 mA. Data were collected within a range of scattering angles (2θs) of 1.5–10°.

An inductively coupled plasma mass spectrometer (ELAN 6100, Perkin Elmer, Waltham, MA) was used to figure out the metal-ion content of the clay.

Transmission electron microscopy (TEM) images were obtained with a TEM 2000 EX-II instrument (JEOL, Tokyo, Japan) operating at an accelerating voltage of 100 kV to observe the nanoscale structure of the various composites. Ultrathin sections were obtained by microtoming with a Super NOVA 655001 instrument glass knife (Leica, Heerbrugg, Switzerland) and subjected to the TEM observation without staining.

The adhesiveness between the silicone rubber sheet and the cured liner was quantified through the peel strength test. The dimensions of the specimen were 20 × 100 ×3 mm^3, and the peel tests were operated at 50 mm/min with a universal testing machine (LR10K, Lloyd Instruments, Bognor Regis, UK).

RESULTS AND DISCUSSION

Clay Modification Process

MMT was modified through cation exchange with 12DA to prepare 12DAC and was subsequently treated with two kinds of amine silanes, namely, APS and Z6020, to yield DAPC and DZC, respectively. The procedure of the modification was followed as shown in Scheme 2.

Figure 1 shows the FTIR spectra of the clays. The doublet peaks at 2870–2840 cm^{-1} in Figure 1(a) corresponded to the asymmetric stretching of the aliphatic chain of 12DA. The same peak was absent in the FTIR spectrum of the pristine MMT; this confirmed the successful modification of MMT by 12DA. In Figure 1(b), the specific peak at 1580–1480 cm^{-1} of DZC caused by NH in-plane deformation vibrations originated from the secondary aliphatic amine groups of Z6020. However, the FTIR spectra did not provide any further information on the structures of the clays because 12DA, APS, and Z6020 had the similar functional groups in their structures.

Table II displays the results of the elemental analyses of the contents of carbon, hydrogen, and nitrogen. The nitrogen content increased with increasing carbon content for all of the clays. DAPC and DZC, which were prepared by the treatment of 12DAC with APS and Z6020, respectively, exhibited higher contents of carbon and nitrogen compared to 12DAC; this confirmed that the amine silanes were successfully incorporated into 12DAC. DZC exhibited the highest content of the three elements, and this indicated that DZC contained the largest amount of the organic compounds.

Figure 2 shows the TGA profiles of MMT, 12DAC, DAPC, and DZC recorded under a nitrogen atmosphere. The modified clays lost more weight than MMT because of the degradation of the incorporated organic compounds. The temperature corresponding to 5% weight loss was 669°C for MMT, whereas those for DAPC and DZC were recorded at 402 and 372 C, respectively. According to the derivative curves of the TGA profiles, MMT exhibited a single maximum peak at 550–700°C, as shown in Figure 2(b), whereas DAPC and DZC exhibited three or more maxima. The multiple maxima were attributed to the degradation of 12DA, APS, and Z6020, which were incorporated into MMT. The maxima in the weight loss rate appearing at temperatures higher than 550°C were due to the loss of water molecules coming from the dehydroxylation of the silanol groups located on the clay surface.[22] The weight loss of DZC was more significant than that of DAPC; this indicated that the amount of Z6020 incorporated into MMT was larger than that of APS. The weight loss recorded at temperatures between 250 and 400°C was attributed to the degradation of the organic parts of DAPC and DZC.

The mass reduction below 100°C should have been due to the evaporation of the absorbed or coordinated water in the clays.

Applied Polymer SCIENCE

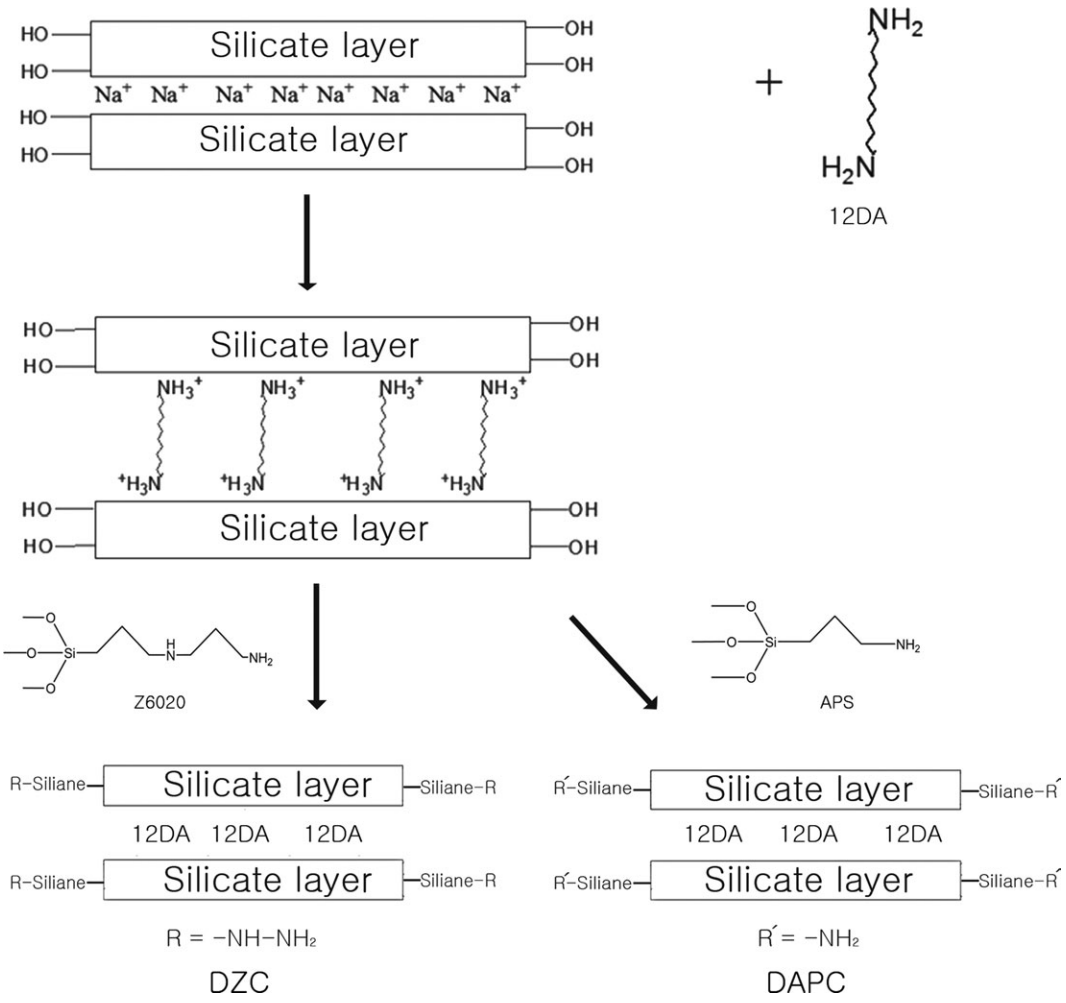

Scheme 2. Clay modification process.

With the dehydroxylation of the silanol groups of the clay surface above 550°C also taken into account, the amount of incorporated organic compounds was calculated from the weight variation between the onset temperature and the tail-end temperature of the weight loss rate peak observed between 150–500°C. The results are summarized in Table III. The amount of organic compounds attached to DZC was larger than that of DAPC; this was in line with the result of the C, H, and N contents shown in Table II.

Figure 3 displays the wide-angle XRD patterns of MMT and the modified clays. The d_{001} spacing was calculated from the peak position with Bragg's law: $2d \sin \theta = n\lambda$, where λ is the wavelength of the X-rays used in the diffraction experiment, d is the spacing between diffracted lattice planes, and θ is the half diffraction angle or glancing angle. MMT shows the specific pattern peak around $2\theta = 7.5°$, whereas the d_{001} peak shifted to $2\theta = 6.46°$ when MMT was modified with 12DA. This revealed that the MMT layers were intercalated with 12DA. The XRD peak position of DZC shifted from 6.46 to 6.1° because of the modification of 12DAC with Z6020, whereas DAPC, which was synthesized by the treatment of 12DAC with APS, showed its XRD peak at the same position as that of 12DAC. With the fact that some of 12DA was released from the interlayer of 12DAC during the treatment of 12DAC with APS and Z6020 taken into account, Z6020 was believed to be inserted into the interlayer of 12DAC at amounts greater than that needed to make up for the loss of 12DA. In contrast, the amount of APS inserted into 12DAC fell short of the amount necessary to compensate for the loss of 12DAC.

The XRD patterns of APC and ZC are also exhibited in Figure 3. APC and ZC were MMT modified with APS and Z6020 in the absence of 12DA, respectively, and thereby they were different from DAPC and DZC in that the latter clays were prepared by the treatment of 12DAC with APS and Z6020, respectively. It was interesting to observe that the XRD peaks of APC and ZC appeared at 6.74 and 6.58°, respectively. When the XRD peak positions of MMT and 12DAC at 7.5 and 6.46°, respectively, were compared, it could be said that APS and Z6020 enlarged the interlayer spacing of MMT as 12DA did because the amine silane compounds plausibly participated in the cationic exchange reaction and permeated the clay interlayer. This was also proven by the Na^+ content of the clays before and after the modification, as summarized in Table IV. The Na^+ contents of APC and ZC were lower than that of MMT; this indicated that some of the Na^+ was replaced by the cationic exchange

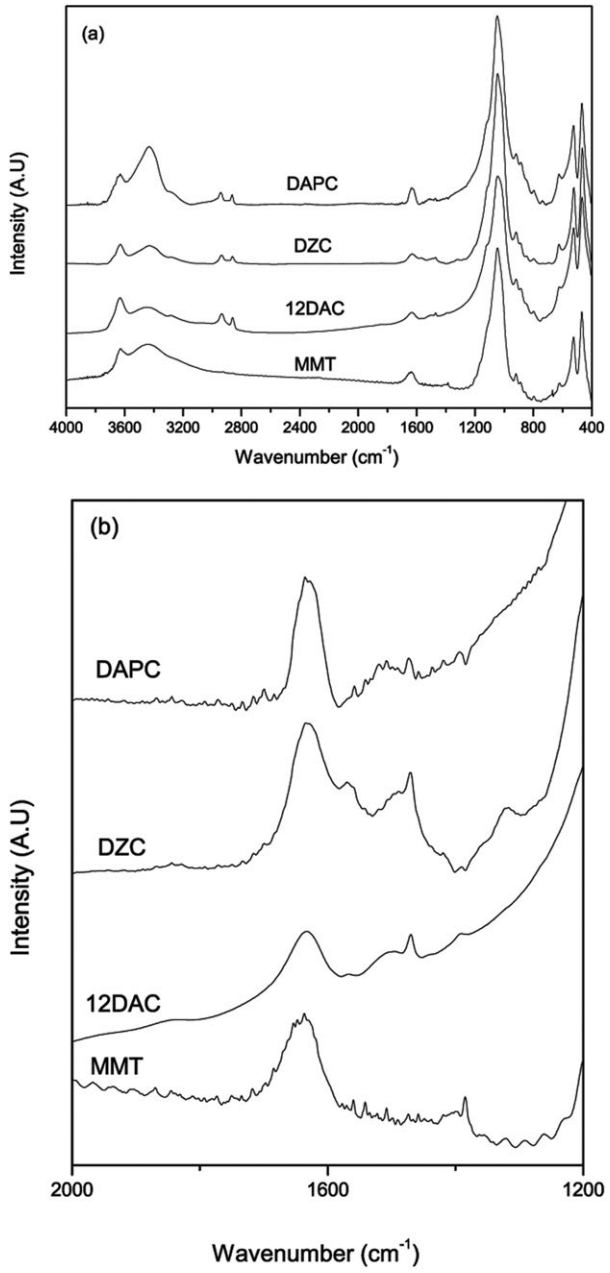

Figure 1. FTIR spectra of the clays.

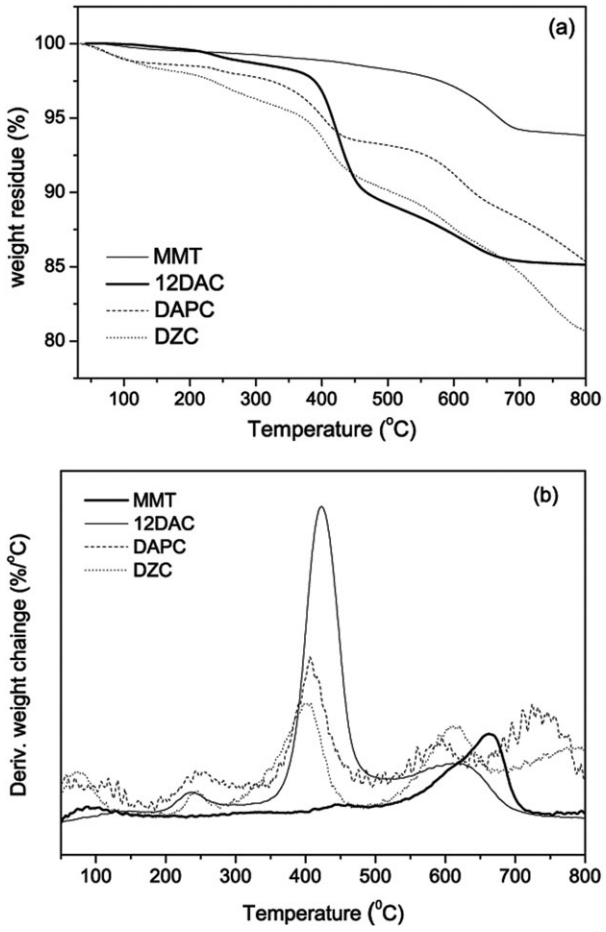

Figure 2. (a) TGA profiles of the clays and (b) derivatives of the TGA profiles.

reactions with APS and Z6020, respectively. The Na^+ content decreased in the order MMT > APC > ZC > 12DAC; this was in line with the results of the degree of the enlargement of the clay layers measured from the XRD patterns. Subramani et al.[23] also observed the clay interlayer enlargement of MMT as a result of modification with Z6020. However, the Na^+ contents of APC and ZC was higher than that of 12DAC; this revealed that the cationic exchanges of APS and Z6020 were less efficient than that of 12DA. DZC possessed the lowest Na^+ content among the clays, and this implied that the Na^+ ions in 12DAC were cation-exchanged further during the treatment with Z6020.

Table II. Results of the Elemental Analyses of the Clays

	Content (wt %)			
Clay	Nitrogen	Carbon	Hydrogen	Total
MMT	0.22	0.22	1.31	1.75
12DAC	1.25	6.43	2.04	9.72
APC	0.65	1.34	1.41	3.40
ZC	0.84	2.05	1.60	4.49
DAPC	1.49	8.69	2.06	12.24
DZC	2.97	15.41	2.49	20.87

Table III. Residual Weight of the Clays Observed during TGA and the Amount of Organic Compounds Attached to the Clays

	W_{T1-T2} (%)	T_1 (°C)	T_2 (°C)	M (g/mol)	Attached amount (mequiv/g)
DAPC	5.10	203.9	464.7	286.74	0.19
DZC	7.63	183.2	481.3	329.77	0.25

T_1, Onset temperature of thermal degradation; T_2, Tail end temperature of thermal degradation; M, Molecular weight; W_{T1-T2}; Weight loss between T_1 and T_2.

Applied Polymer SCIENCE

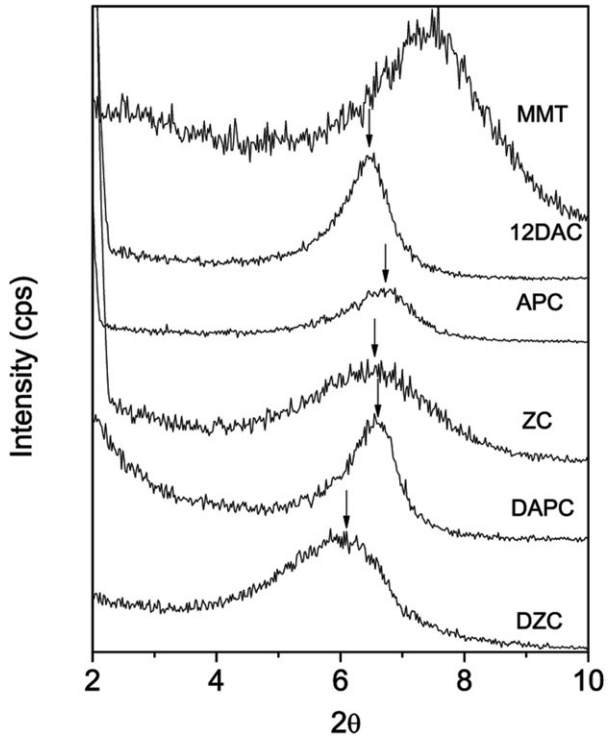

Figure 3. XRD patterns of the clays.

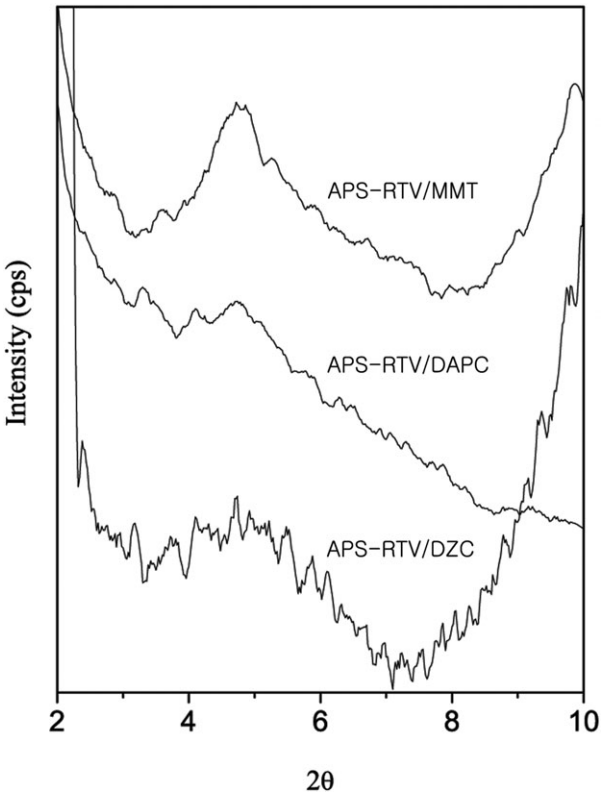

Figure 4. XRD patterns of the APS–RTV/clay nanocomposites.

However, it was curious that the Na^+ content of DAPC was almost the same as that of DZC even though the interlayer spacing of DAPC was narrower than that of DZC, as compared in Figure 3. This may have been due to the less bulky molecular structure of APS compared to that of 12DA and Z6020, which meant that the interlayer enlargement by the former silane was less effective than those by the latter two compounds.

Morphology of the APS–RTV/Clay Composites

Figure 4 shows the XRD patterns of the APS–RTV/MMT, APS–RTV/DAPC, and APS–RTV/DZC composites. The compounding of MMT with APS–RTV moved the d_{001} peak from $2\theta = 7.5$ to 4.78°; this revealed that APS–RTV molecules were inserted into the MMT layers. The d_{001} peak of DZC shifted from $2\theta = 6.5$ to 4.72° when DZC was compounded with APS–RTV. Furthermore, the diffraction peak at $2\theta = 4.46°$ of APS–RTV/DAPC was less intense than that of APS–RTV/MMT.

The d_{001} peak of the APS–RTV/MMT composite appeared at similar angle to that of APS-RTV/DZC, even though MMT was not modified at all. This was ascribed to the fact that the silanol groups of MMT participated in the condensation reaction during the APS–RTV preparation.

Table IV. Na^+ Contents of the Clays

Clay	Na^+ Content (wt %)
MMT	1.49 (±0.0220)
12DAC	0.28 (±0.0025)
APC	1.02 (±0.0077)
ZC	0.78 (±0.0052)
DAPC	0.12 (±0.0015)
DZC	0.13 (±0.0010)

A nanometer-scale dispersion of the neat and modified clays within the APS–RTV matrix could be observed in the TEM images shown in Figure 5. The spaces between the black lines represents the galley interlayer of the clays, whereas the bright background corresponds to the APS–RTV matrix. In case of the APS–RTV/MMT composite, the clay platelets appeared at regular intervals, as shown in Figure 5(a). In line with the results in Figure 4, the APS–RTV/MMT composite demonstrated an intercalated morphology without a discernible collapse of the stacked layers of MMT. The low-molecular-weight APS–RTV molecules might have swelled the MMT layers in the initial stage and helped the APS–RTV molecules to penetrate the clay layers. The APS–RTV molecules remaining embedded in the clay layers during the curing process yielded an APS–RTV/MMT composite with intercalated morphology. The reaction between the silanol groups located at the clay edges and the silanol groups of APS–RTV during the composite preparation should have also contributed to the enhancement of the compatibility between APS–RTV and MMT. DAPC and DZC had lower hydroxyl groups on the edge because of the exhaustion of the hydroxyl groups during the grafting of the amine silanes. However, the bigger gap of the modified clays compared to that of MMT should have facilitated the permeation of the APS–RTV precursors into the clay gallery [see Figure 5(b,c)].

Adhesion Properties of the APS–RTV/Clay Composites

APS–RTV was prepared by the copolymerization of dimethyl siloxane with APS to improve the adhesion between the silicone

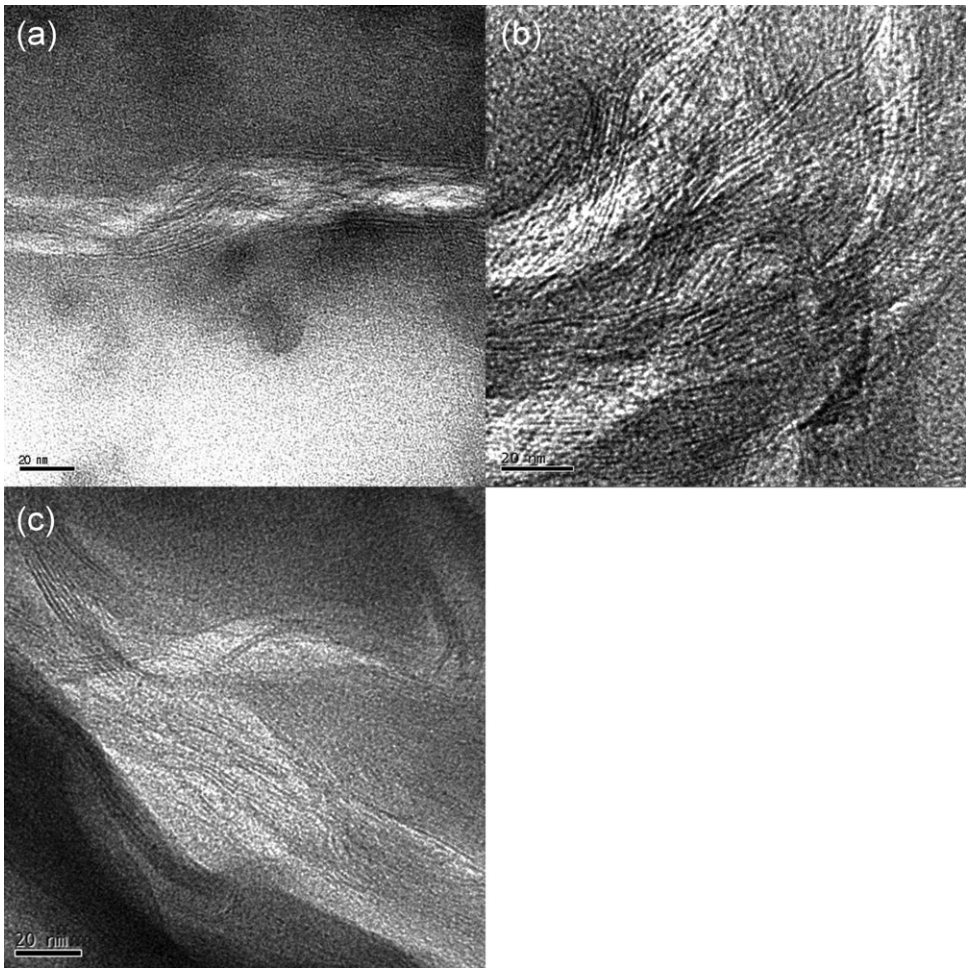

Figure 5. TEM image of the APS–RTV/clay composites: (a) APS–RTV/MMT, (b) APS–RTV/DAPC, and (c) APSRTV/DZC.

rubber and the liner sheet. The liner was prepared by the spreading and curing of the liner components, composed of HTPB, DDI, and FeAA, on the sheet made of the APS–RTV/clay composites. The chemical reaction should have occurred between the isocyanate groups in the liner components and the amine groups in APS–RTV, as shown in Scheme 3.

Peeling tests were performed according to ASTM 1876-01, and the peel strength (P_s; N/m) was determined with eq. (1):

$$P_s = \frac{F}{t} \tag{1}$$

where F is adhesion force (N) and t is the width of the specimen (cm). The results of the peeling tests are summarized in Table V.

RTV without any amine groups showed a peel strength of 0 N/cm; this indicated that the chemical reaction between the amine groups and the isocyanate groups of the liner was essential for the enhancement of the adhesion.

Aging the APS–RTV/liner laminates further raised the peel strength in that the APS–RTV/liner laminate resulted in a 3.7 N/m peel strength, whereas the value rose to 4.4 when the same laminate was aged at room temperature for 1 week.

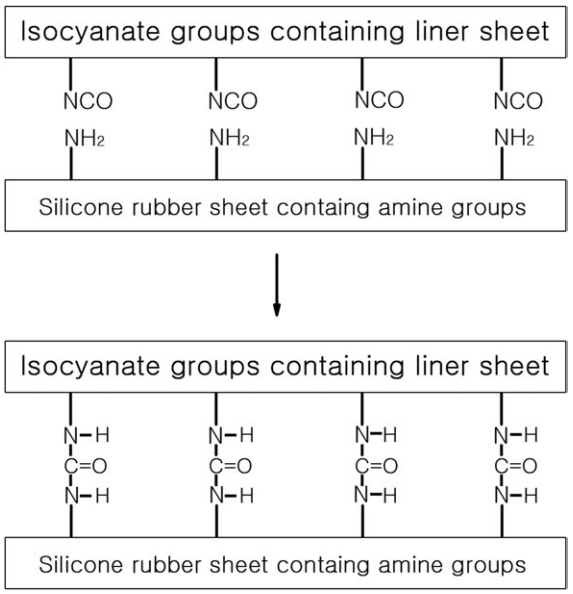

Scheme 3. Plausible chemical reaction between the RTV and the liner.

Table V. Peel Strength of the APS–RTV/Clay Composites

Composite	Peel strength (N/cm)
RTV (without APS)	0
APS-RTV	3.7
APS-RTV (aged for a week)	>4.4[a]
APS-RTV/MMT	2.8
APS-RTV/DAPC	>5.7[a]
APS-RTV/DZC	4.1

[a]The silicone rubber adhered to the liner so strongly that the silicone rubber sheet was torn off during the peeling test.

The adhesion force decreased slightly when MMT was compounded with APS–RTV; this indicated that addition of MMT was not helpful for the enhancement of the adhesion force. However, the incorporation of DAPC improved the adhesion force so effectively that the silicone sheet was torn off rather than delaminated from the liner sheet during the peeling test. The enhanced adhesion force of APS–RTV/DAPC was ascribed to the additional interfacial chemical reaction between the isocyanate groups of the liner components and the amine groups of APS grafted to MMT. However, APS–RTV/DZC exhibited a higher adhesion force than APS–RTV and APS–RTV/MMT, but the adhesion force was lower than that of APS–RTV/DAPC. This was contrary to our expectations because the amount of Z6020 incorporated into DZC was larger than that of APS incorporated into DAPC, and thereby, the content of the amine groups in DZC available for the reaction with the liner components should have been higher than that in DAPC. Because the interfacial interaction is crucial for the adhesion, further study is needed to characterize the amine group content at the interface to determine a clear explanation for why APS–RTV/DZC had a lower adhesion force than APS–RTV/DAPC.

CONCLUSIONS

APS–RTV was prepared by the copolymerization of dimethyl siloxane with APS to improve the adhesion force between the silicone rubber and the liner sheet containing isocyanate groups. 12DAC, which was MMT modified with 12DA, was treated further with APS and Z6020 to produce DAPC and DZC, respectively. The TGA weight loss of DZC was more significant and its interlayer spacing was wider than that of DAPC; this indicated that the amount of Z6020 incorporated into the clay was larger than that of APS. APS and Z6020 were also intercalated into the MMT layers through the cationic exchange reaction. Not only the d_{001} peak of the modified clays but also that of the neat clay moved to a lower angle as a result of the compounding of APS–RTV; this revealed that the APS–RTV molecules were inserted into the clay layers and cured. APS–RTV/DAPC showed the highest adhesion force between the silicone rubber and the liner sheet among the tested composites because of the contribution of DAPC to the reaction with the isocyanate groups of the liner component.

ACKNOWLEDGMENT

This work was supported by Inha University.

REFERENCES

1. Fan, J. L.; Ho, W. D. U.S. Pat. Appl. 20050054754, A1 (**2005**).
2. Wong, J. L.; Johnson, G. P. U.S. Pat. 6,486,233, B1 (**2002**).
3. Grythe, K. F.; Hansen, F. K.; Olsen, T. J. *J. Adhes.* **2007**, *83*, 223.
4. Moraes, J. H.; da Silva Sobrinho, A. S.; Maciel, H. S.; Dutra, J. C. N.; Massi, M.; Mello, S. A. C. *J. Phys. D: Appl. Phys.* **2007**, *40*, 7747.
5. Youren, J. W. *Composites* **1971**, *2*, 180.
6. Khan, M. B. *Polym.-Plast. Tech. Eng.* **1996**, *35*, 187.
7. Jia, X. L.; Li, G.; Sui, G.; Li, P.; Yu, Y. H.; Liu, H. Y. *Mater. Chem. Phys.* **2008**, *112*, 823.
8. Mark, J. E.; Ngai, K.; Graessley, W.; Mandelkern, L.; Samulski, E.; Koenig, J. Physical Properties of Polymers, 3rd ed.; Cambridge University: Cambridge, United Kingdom, **2003**.
9. Mark, J. E.; Allcock, H. R.; West, R. Inorganic Polymers; Prentice Hall: Englewood Cliffs, NJ, **1992**.
10. Clarson, S. J.; Semlyen, J. A. Siloxane Polymers; Prentice Hall: Englewood Cliffs, NJ, **1993**.
11. Noll, W. The Chemistry and Technology of Silicones; Academic: New York, **1968**.
12. Olsen, T. O. U.S. Pat. 4,297,265 (**1981**).
13. Peignot, P.; Rhodes, K. *Med. Device Technol.* **2004**, *15*, 22.
14. Bobear, W. J. U.S. Pat. 3,723,481 (**1973**).
15. Dittman, D. O.; Licari, J. J.; Michael, G. U.S. Pat. 3,380,941 (**1968**).
16. Kim, E. S.; Kim, H. S.; Jung, S. H.; Yoon, J. S. *J. Appl. Polym. Sci.* **2007**, *103*, 2782.
17. Zhu, J.; Morgan, A. B.; Lamelas, F. J.; Wilkie, C. A. *Chem. Mater.* **2001**, *13*, 3774.
18. Jeon, H. G.; Jung, H. T.; Lee, S. W.; Hudson, S. D. *Polym. Bull.* **1995**, *41*, 107.
19. Furuichi, N.; Kurokawa, Y.; Fujita, K.; Oya, A.; Yasuda, H.; Kiso, M. *J. Mater. Sci.* **1996**, *31*, 4307.
20. Heinemann, J.; Reichert, P.; Thomann, R.; Mulhaupt, R. *Macromol. Rapid Commun.* **1999**, *20*, 423.
21. Shim, J. H.; Kim, E. S.; Joo, J. H.; Yoon, J. S. *J. Appl. Polym. Sci.* **2006**, *102*, 4983.
22. Frost, R. L.; Kristof, J.; Horvath, E.; Kloprogge, J. T. *Langmuir* **2001**, *17*, 3216.
23. Subramani, S.; Choi, S. W.; Lee, J. Y.; Kim, J. H. *Polymer* **2007**, *48*, 4691.